The light and shade of perovskite solar cells

Michael Grätzel

The rise of metal halide perovskites as light harvesters has stunned the photovoltaic community. As the efficiency race continues, questions on the control of the performance of perovskite solar cells and on its characterization are being addressed.

Alkali-metal lead and tin halides had been synthesized already in 1893[1], yet the first crystallographic studies that determined that caesium lead halides had a perovskite structure with the chemical formula $CsPbX_3$ (X = Cl, Br or I) were only carried out 64 years later by the Danish scientist Christian Møller[2]. He also observed that these coloured materials were photoconductive, thus suggesting that they behave as semiconductors. In 1978, Dieter Weber replaced caesium with methylammonium cations ($CH_3NH_3^+$) to generate the first three-dimensional organic–inorganic hybrid perovskites[3,4]. The general crystal structure of these materials is shown in Fig. 1. Caesium ions or small organic cations such as methylammonium and formamidinium occupy the cuboctahedral voids formed by the 12 nearest-neighbour halide ions. The structural characterization of hybrid perovskites of the formula $CH_3NH_3BX_3$ (with B = Sn(II) or Pb(II), and X = Cl, Br or I) has also been reviewed in more recent studies[5].

Methylammonium lead iodide, $CH_3NH_3PbI_3$, has both interesting optical and electronic properties that have been actively investigated during the past two decades[5–7]. It is a semiconducting pigment with a direct bandgap of 1.55 eV corresponding to an absorption onset of 800 nm (ref. 6), which makes this material a good light absorber over the whole visible solar emission spectrum. The excitons produced by light absorption have a weak binding energy of about 0.030 eV, which means that most of them dissociate very rapidly into free carriers at room temperature[8]. The electrons and holes produced in this material exhibit a small effective mass[9] resulting in high carrier mobilities that range from 7.5 $cm^2 V^{-1} s^{-1}$ for electrons[9] to 12.5 $cm^2 V^{-1} s^{-1}$ – 66 $cm^2 V^{-1} s^{-1}$ for holes[10]. Their recombination occurs on a timescale of hundreds of nanoseconds, resulting in long carrier-diffusion lengths — that is, the average distance that can be covered by carriers before they recombine — ranging between 100 nm and 1,000 nm (refs 11,12). Despite some of these appealing properties that were already known for more than 20 years, the extraordinary potential of hybrid perovskites in photovoltaic applications was only revealed less than 5 years ago by researchers working on liquid-electrolyte-based dye-sensitized solar cells (DSSCs)[13,14]. These two papers and the three publications[15–17] that followed in 2012, reporting on the use of tin or lead iodide perovskites in a solid-state version of the DSSC, set off the current meteoric rise of perovskite solar cells (PSCs).

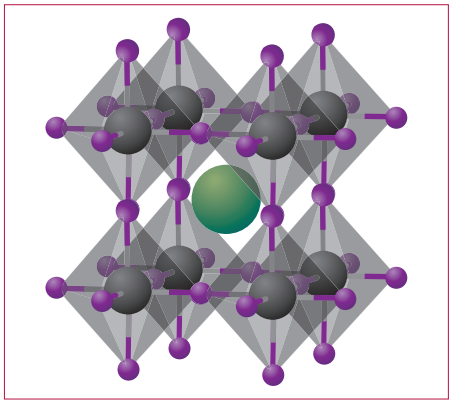

Figure 1 | Crystal structure of cubic metal halide perovskites with the generic chemical formula ABX_3. Organic or inorganic cations occupy position A (green) whereas metal cations and halides occupy the B (grey) and X (purple) positions, respectively.

Ascension of perovskite solar cells

In 2009, when Kojima *et al.* introduced $CH_3NH_3PbI_3$ and the larger-bandgap analogue $CH_3NH_3PbBr_3$ as sensitizers for liquid-electrolyte-based DSSCs[13], the power-conversion efficiency (PCE) measured under standard characterization conditions reached a mere 3.8%, and the device stability was poor due to the rapid dissolution of the perovskite in the organic solvent. However, by changing both the electrolyte formulation and the method of depositing the perovskite, the group of Nam-Gyu Park was able to increase the device performance and stability attaining a PCE of 6.5%[14]. The authors noted that $CH_3NH_3PbI_3$ was a superior light harvester compared with the more commonly used molecular N719 ruthenium sensitizer, meaning that a thinner absorbing layer was sufficient to obtain good light-conversion performance.

A key advance was subsequently made by replacing the liquid electrolyte with a solid-state hole conductor (or hole-transporting material, HTM), that is, $CsSnI_{3-x}F_x$ (ref. 15) or spiro-MeOTAD[16,17]. Not only did the conversion efficiency double, but the cell stability also improved greatly as a result of avoiding the use of a liquid solvent. At this stage, the embodiment of the PSC was an exact mimic of the solid-state DSSCs (Fig. 2). The N719 dye[15] or the $CH_3NH_3PbI_3$ perovskite nanoparticles[16,17] assume the role of the sensitizer injecting electrons in a mesoscopic TiO_2 scaffold and holes in a solid-state HTM. Both the TiO_2 and the HTM act as selective contacts through which the charge carriers produced by photoexcitation of the perovskite nanoparticles are extracted.

A change in paradigm occurred with the discovery by Lee *et al.*[17] that a mesoporous scaffold made of Al_2O_3 instead of TiO_2 produced similar — if not better — conversion efficiencies, even though Al_2O_3 is unable to assist in electron extraction due to its large bandgap. This suggested that the perovskite itself transported the electrons

to the front collector electrode composed of a compact blocking layer of TiO_2 deposited on a fluorine-doped tin oxide conducting glass (Fig. 3a). These researchers proposed that the electrons percolate along the surface of the Al_2O_3 nanoparticles through an ultrathin conformal coating of $CH_3NH_3PbI_3$. However, until now, the role — if any — of the mesoscopic Al_2O_3 scaffold in these devices, for which the term 'meso-superstructured' has been coined, remains obscure.

At the same time, it became clear from the studies of Etgar *et al.*[18] that $CH_3NH_3PbI_3$ could also assume the role of a hole conductor, obviating the need for employing an additional HTM. Although the initial conversion efficiency for these 'HTM-free' architectures was only about 5%, it has been growing steadily over the past two years. Today, PSC embodiments based on HTM-free mesoscopic $CH_3NH_3PbI_3/TiO_2$ heterojunctions that use a double layer of TiO_2 and ZrO_2 as scaffold, and carbon as a back contact have reached a certified PCE of 12.8% and — contrary to many HTM-based PSCs — exhibit excellent stability under long-term light soaking[19].

The finding that $CH_3NH_3PbI_3$ can act as a hole conductor in a PSC prompted a new development culminating in the realization of nanocomposite solar cells[20], where the TiO_2 scaffold is fully infiltrated with the perovskite light harvester (Fig. 3b). This allowed the mesoscopic $CH_3NH_3PbI_3/TiO_2$ film thickness to be reduced to 200–300 nm without sacrificing photocurrent. Note that this PSC configuration featured a poly(triarylamine) HTM instead of the previously employed spiro-MeOTAD[20]. Application of energy-dispersive spectroscopy and X-ray diffraction depth profiling confirmed that the pores of the TiO_2 film were fully infiltrated with the $CH_3NH_3PbI_3$, whereas the poly(triarylamine) penetrated the scaffold to a much smaller degree. A high PCE of 12% was achieved, suggesting that the carrier collection by hole transport through the perovskite was very effective. Transistor measurements confirmed that $CH_3NH_3PbI_3$ behaved as an ambipolar semiconductor, being able to transport both electrons and holes in keeping with the results of Lee *et al.*[17] and Etgar and colleagues[18]. This paved the way towards PSC configurations with a planar geometry[21,22], as shown in Fig. 3c.

Engineering the deposition process

The results described previously relied on the single-step deposition of the perovskite pigment using a mixture of PbX_2 and CH_3NH_3X (X = Cl, Br or I) from a common solvent such as γ-butyrolactone, dimethylformamide or dimethylsulphoxide. However, this approach typically led to uncontrolled morphological variations, which resulted in poor reproducibility of photovoltaic performance. To gain a better control of the crystal formation and growth a sequential deposition method was developed[23]. Lead iodide (PbI_2) was first loaded by spin coating from dimethylformamide onto the mesoporous titanium dioxide film and then exposed to a solution of CH_3NH_3I in isopropanol; this led to the formation of the final perovskite pigment penetrating the porous titania film. Strikingly, on the mesoscopic length scale the conversion occurred within seconds and permitted much better control over the perovskite morphology than with the single-step route. An image of the cross-section of the device is shown in Fig. 4. This technique greatly increased the reproducibility of the solar cell's performance and boosted the PCE to 15%. Subsequently, the PCE of a perovskite photovoltaic cell prepared by a modified two-step procedure was certified to be 15.45%.

Much progress has also been made in the preparation of planar PSCs, where various methods have been applied ranging from dual-source high-vacuum evaporation[21,22] to sequential liquid–vapour phase deposition[24] and low-temperature solution casting[25].

Today, the best-performing cells have reached a certified PCE of 17.9%, which is more than four times higher than the value attained in 2009; an unprecedented and stunning rise in efficiency for a photovoltaic technology. The group of Sang Il Seok has achieved these latest advances by judicious selection of solvent mixtures based on γ-butyrolactone, dimethylsulphoxide and toluene to control the nucleation of $CH_3NH_3PbI_3$ crystals within the mesoporous TiO_2 scaffold and the subsequent growth of a dense $CH_3NH_3PbI_3$ capping layer. The latter plays a crucial role in enhancing the absorption of photons by the perovskite in the wavelength region above 550 nm, thus substantially increasing the photocurrent. In this issue of *Nature Materials* is an Article by this group[26] in which they describe in detail their method of solvent-controlled crystal-growth engineering used to attain these high PCE values.

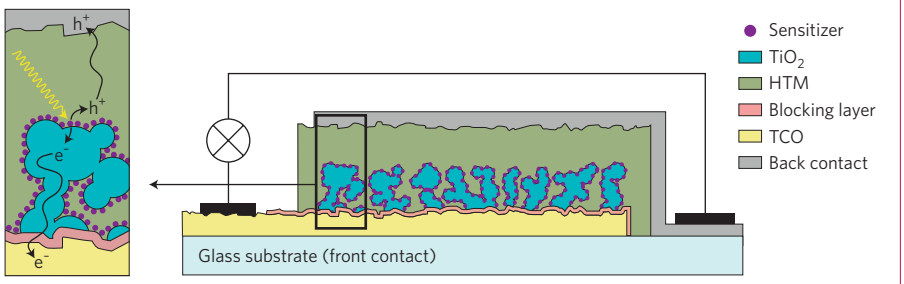

Figure 2 | Schematic cross-section of a solid-state mesoscopic solar cell using N719 or $CH_3NH_3PbI_3$ as a sensitizer. The perovskite nanoparticles are precipitated from solution onto a mesoscopic TiO_2 film acting as an electron-extraction layer. Spiro-MeOTAD was mostly used as an HTM[16,17]. The external electric circuit contacting the solar cell is shown in black. In the close-up view on the left, the light radiation (yellow wavy arrow) hitting the sensitizer generates electrons (e^-) and holes (h^+) that are transported in the TiO_2 and HTM layers, respectively. TCO, transparent conducting tin oxide layer.

More exciting discoveries

The recent intense research efforts have unravelled some extraordinary properties of these metal halide perovskites. For instance, a giant low-frequency dielectric constant exceeding 1 million was recently observed in $CH_3NH_3PbI_3$ films under illumination, whereas the value was 1,000 times smaller in the dark[27]. As a consequence of the high dielectric constant, these materials show a very large capacitance that is likely to be the cause of the slow impedance response in the mHz frequency range observed with these systems[28]. The observation of a giant dielectric constant suggests that a very strong polarization of the perovskite lattice occurs in response to the electric field, that is, the photovoltage, which is generated under illumination. This polarization is likely to originate from the displacement of $CH_3NH_3^+$ cations, which is also at the origin of the ionic conductivity of metal halide perovskites[10,29]. As a consequence of the displacement, ion-induced screening of the Coulombic attraction between the charge carriers generated by light is enhanced and electrons and holes can separate more

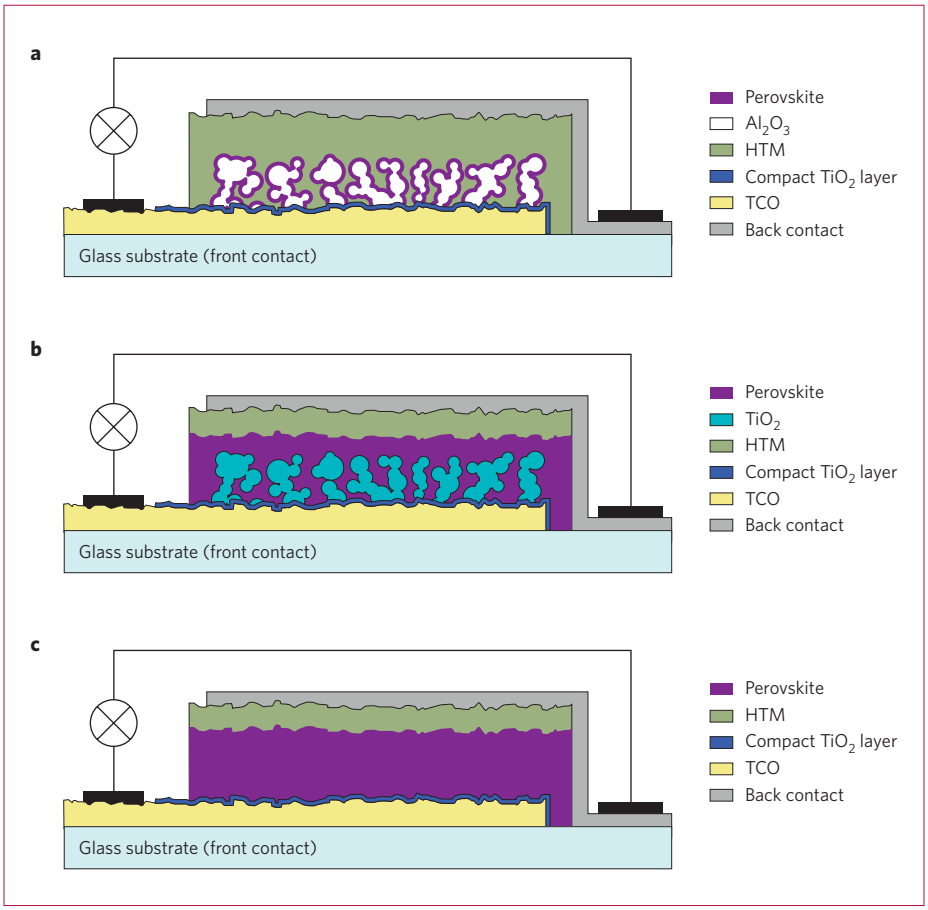

Figure 3 | Evolution from a mesoscopic to a planar embodiment of the perovskite solar cell. **a**, 'Meso-superstructured' PSC employing a film of Al_2O_3 nanocrystals covered with a conformal overlayer of $CH_3NH_3PbI_3$ perovskite. The latter acts as a light harvester as well as an electron conductor. **b**, Nanocomposite embodiment of a PSC where the mesoscopic TiO_2 scaffold is infiltrated by the perovskite. The perovskite assumes the dual role of light absorber and hole conductor. The structure is akin to p–i–n solar cells. **c**, Cross-section of a planar heterojunction solar cell lacking the TiO_2 mesoporous scaffold.

easily; this leads to a net improvement of the performance of PSCs. A similar screening effect is also operative in DSSCs where it arises from ions present at the interface of the nanocrystalline TiO_2 film with the electrolyte[30].

Films of $CH_3NH_3PbI_3$ also exhibit lasing at surprisingly low optical pumping thresholds, indicating a high level of crystallinity and small concentration of bulk impurities or defects in the perovskite material[31,32]. As a consequence, the radiationless decay of excitons that shortens their lifetime seems to be mainly controlled by surface states[31]. This is astonishing in view of the fact that the films are prepared by solution processing, which usually engenders a large concentration of bulk defects. High-quality crystalline perovskite layers that are suitable for laser applications can therefore be obtained by low-cost deposition methods. A further advantage of metal halide perovskite lasers is their wide tunability over the visible range, which is readily achieved by replacing the iodide with bromide ions.

The characterization of the electroluminescence properties of fully operational PSCs allowed further insight to be gained on the rather high open-circuit photovoltage, V_{OC}, observed in these devices, typically ranging between 0.9 V and 1.15 V. Owing to entropic losses, the maximum obtainable V_{OC} of solar cells measured under standard characterization conditions is about 300 mV below the bandgap. Hence, for $CH_3NH_3PbI_3$ with a bandgap of 1.55 V the maximum V_{OC} is 1.25 V. However, as explained theoretically by Robert Ross in 1967[33], this ideal value, $V_{OC\text{-}ideal}$, is reached only if the external quantum efficiency, η_{ext}, of the light emission by the solar cell measured at V_{OC} is 100%. Each decrease in η_{ext} by a factor of 10 will entail a 60-mV loss in V_{OC} according to the formula:

$$V_{OC} = V_{OC\text{-ideal}} + (kT/q)\ln(\eta_{ext}) \qquad (1)$$

where k is the Boltzmann constant, T is temperature, q is the elementary charge and η_{ext} is the external quantum efficiency of the photovoltaic cell at V_{OC} obtained under standard measurement conditions. In line with these theoretical predictions the electroluminescence quantum yield of PSCs has been found to correlate with its V_{OC} (W. Tress, N. Marinova, O. Inganäs, M. K. Nazeeruddin, S. M. Zakeeruddin and M. G., manuscript submitted for publication).

Open issues and pitfalls

During the impending phase of consolidation, a number of questions concerning the true potential of PSCs for widespread deployment will have to be addressed.

Stability. Very few stability studies have been performed so far[19,23] and at this stage it is unclear whether PSCs can meet the stringent international norms for outdoor photovoltaic applications. Therefore, extensive stability tests are urgently warranted. These include long-term light-soaking tests (1,000 h in full sunlight) as well as damp heat tests (1,000 h at 85% humidity and 85 °C). It is well known that $CH_3NH_3PbI_3$ degrades in humid conditions and forms PbI_2 at higher temperatures due to the loss of CH_3NH_3I. These instabilities could hamper outdoor applications.

Toxicity. Lead compounds are very toxic and harmful to the environment. The health risks and dangers of $CH_3NH_3PbI_3$ are currently being investigated by a consortium of experts within the framework of the integrated European Joule 7 project Future Nano-Needs (FNN). $CH_3NH_3PbI_3$ in contact with polar solvents such as water can convert to PbI_2, a carcinogen, that is moderately water-soluble and whose use is banned in many countries. Therefore it seems that identifying lead-free perovskites or other pigments that can replace $CH_3NH_3PbI_3$ is necessary for the widespread deployment of PSCs. The tin analogues $CH_3NH_3SnI_3$ (refs 34,35) and $CsSnI_3$ (ref. 36) show promise, but their extreme sensitivity to oxygen presents a severe caveat that will have to be addressed to enable practical applications.

Pitfalls in measuring conversion efficiencies. The appearance in the photocurrent–voltage curves of strong

hysteresis — which consists of the anomalous dependence of the PCE on the voltage scan direction and speed — calls into question published PCE values that have not been certified. The results by Seok *et al.*[26] show that the hysteresis effect is particularly severe for planar device configurations. Hence, PCE values previously reported in literature for planar architectures should be carefully checked. The authors also show the appearance of hysteresis for thicker mesoporous TiO_2 layers. In this case, however, it has been reported that by reducing the voltage scan speed it is possible to fully suppress this anomalous behaviour even in solar cells having 3-μm-thick mesoscopic oxide scaffolds[19]. Independently of the cell embodiment used, it is good practice to carefully verify the presence of any hysteresis by collecting the photocurrent–voltage curves in both forward and reverse voltage scanning directions and as a function of scanning speed. Failure to do so leads to large overestimations of the device PCE[26,28]. A further source of error lies in measuring cell efficiencies on devices smaller than 0.1 cm^2. It has been shown that for such small cells optical artefacts can inflate the values of the short-circuit photocurrent[37].

Doping of $CH_3NH_3PbI_3$ with chloride ions. It has been suggested that replacing PbI_2 with $PbCl_2$ as a starting material to form $CH_3NH_3PbI_3$ can lead to doping of the perovskite structure with chloride ions[17]. However, no chloride ions could be detected in the $CH_3NH_3PbI_3$ crystals formed during the reaction despite extensive analytical efforts. Based on careful X-ray diffraction and elemental analysis, the group of Peter Erk has recently confirmed the absence of any chloride doping in $CH_3NH_3PbI_3$ crystals formed from $PbCl_2$ in this manner (keynote lecture, 6th International Conference on Hybrid and Organic Photovoltaics, HOPV 14, 11–14 May 2014, Lausanne Switzerland). Instead of substituting iodide in the $CH_3NH_3PbI_3$ lattice, the chloride ions become part of an amorphous lead-containing phase that melts at around 103 °C. In view of these unambiguous results, the use of formulas such as $CH_3NH_3PbI_{3-x}Cl_x$ to indicate a chloride-doped state of the lead iodide perovskite is no longer justifiable and should be avoided.

Planar versus mesoscopic architectures

The simple structure of the planar embodiment for a PSC shown in Fig. 3c suggests that ultimately all devices may adopt this configuration. However, at present, mesoscopic systems with a certified PCE of 17.9% have a large lead over planar embodiments, whose reported efficiencies are inferior to this record and remain uncertified so far. Moreover, as pointed out above, the hysteresis issue calls into question the reported PCE values for planar devices. The use of a mesoporous TiO_2 scaffold to host the perovskite material strongly attenuates the hysteresis effects and increases dramatically the carrier-collection efficiency, which is given by equation (2):

$$\eta_{coll} = (1 + (d/L_D)^2)^{-1} \quad (2)$$

where d^2 is the mean square displacement necessary for an electron (or exciton) to reach the perovskite/TiO_2 interface from the point where it is photogenerated, and L_D is the diffusion length. The mesoporous architecture typically reduces d to less than 10 nm, which means that a diffusion length of 100 nm (ref. 11) would be enough to reach a carrier-collection efficiency higher than 99%. By contrast, for a planar film with a thickness of 250 nm — which corresponds to the minimum $CH_3NH_3PbI_3$ thickness to achieve good optical absorption of photons in the 600–700 nm wavelength range, where the solar photon flux is most intense — the collection efficiency would be less than 50%. Thus the prime advantage of the mesoscopic PSC embodiment over the planar configuration is that it can reach carrier-collection efficiencies (and therefore external quantum efficiencies for photocurrent generation) close to 100%, even with systems where the exciton or charge-carrier diffusion length is much shorter than the photon absorption length. This has been confirmed in a recent study by Noel *et al.*[35] on PSCs using tin perovskites as a light harvester. Whereas on Al_2O_3 the $CH_3NH_3SnI_3$ gave a negligible photovoltaic output, with the TiO_2 scaffold a maximum PCE of 6.4% was obtained. Importantly, the V_{OC} = 0.88 V measured with the $CH_3NH_3SnI_3/TiO_2$ nanocomposite was only 350 mV below the bandgap energy, approaching the V_{OC_ideal} value of 0.93 V for $CH_3NH_3SnI_3$. According to equation (1), this implies that the external quantum efficiency for luminescence at V_{OC} should be about 10%, which is high for a device exhibiting carrier lifetimes in the picosecond time domain. The fact that V_{OC} values near the theoretical limit can be reached with $CH_3NH_3SnI_3/TiO_2$ nanocomposites clearly shows that, contrary to a contention expressed earlier[17], employing a mesoporous TiO_2 scaffold does not necessarily entail a loss in V_{OC}.

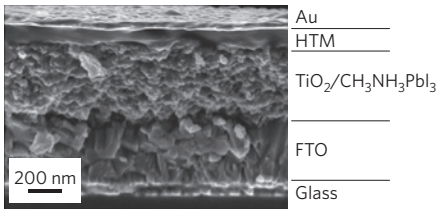

Figure 4 | Cross-sectional scanning electron microscopy picture of a mesoscopic perovskite solar cell prepared by the sequential deposition method. $CH_3NH_3PbI_3$ densely infiltrates the TiO_2 scaffold and forms an interpenetrating network junction on the nanometre length scale. FTO, fluorine-doped tin oxide. Figure reprinted from ref. 23, Nature Publishing Group.

Finally, it should be noted that the line between planar and mesoscopic cell configurations is often difficult to draw. Frequently 'planar' embodiments are supported on a nanocrystalline film of TiO_2, ZnO or the C_{60} derivative [6,6]-phenyl-C_{61}-butyric acid methyl ester (PCBM) as an electron-capture layer. Also, planar perovskite films are often porous, especially if they are made by solution-processing at low temperatures and hence can form mesoscopic junctions with the hole conductor. On the other hand, the efficiency of PSCs based on mesoscopic TiO_2 scaffolds is boosted by placing a compact perovskite overlayer on top of the $CH_3NH_3PbI_3/TiO_2$ nanocomposite[26]. Thus, it may well be that a marriage of the planar and mesoscopic architecture will win in the end.

Outlook

At present, the PSC field is in a dynamic state and reports on further improvements in performance are expected in the near future, where reaching a PCE of 20% seems now to be a realistic goal. Furthermore, PSCs are attractive candidates for use as top cells in two-level tandem configurations using crystalline silicon or copper indium gallium selenide-based photovoltaic devices as bottom cells. For silicon-based tandems, PCEs of 28% to 30% seem to be feasible. However, large-scale deployment of perovskite cells will depend on whether stability and toxicity issues can be solved. The amazing advances made recently with perovskite photovoltaics will undoubtedly spur researchers to expand their investigations to other inorganic or organic pigments, for which the power of mesoscopic solar-cell architectures offers new and promising opportunities. ❐

Michael Grätzel is at the Laboratory of Photonics and Interfaces, Swiss Federal Institute of Technology, CH-1015 Lausanne, Switzerland.
e-mail: michael.graetzel@epfl.ch

References

1. Wells, H. L. *Z. Anorg. Chem.* **3,** 195–210 (1893).
2. Møller, C. K. *Nature* **182,** 1436 (1958).
3. Weber, D. *Z. Naturforsch.* **33b,** 1443–1445 (1978).
4. Weber, D. *Z. Naturforsch.* **33b,** 862–865 (1978).
5. Mitzi, D. B. *Synthesis, Structure and Properties of Organic–Inorganic Perovskites and Related Materials: Progress in Inorganic Chemistry* Vol. 48 (ed. Karlin, K. D.) 1–121 (J. Wiley & Sons, 1999).
6. Baikie, T. *et al. J. Mater. Chem. A* **1,** 5628–5641 (2013).
7. Umari, P., Mosconi, E. & De Angelis, F. Preprint available at http://arxiv-web.arxiv.org/abs/1309.4895 (2013).
8. Ponseca, C. S. *et al. J. Am. Chem. Soc.* **136,** 5189–5192 (2014).
9. Mitzi, D. B. *J. Chem. Soc. Dalton Trans.* **1,** 1–12 (2001).
10. Stoumpos, C. C., Malliakas, C. D. & Kanatzidis, M. G. *Inorg. Chem.* **52,** 9019–9038 (2013).
11. Xing, G. C. *et al. Science* **342,** 344–347 (2013).
12. Stranks, S. D. *et al. Science* **342,** 341–344 (2013).
13. Kojima, A., Teshima, K., Shirai, Y. & Miyasaka, T. *J. Am. Chem. Soc.* **131,** 6050–6051 (2009).
14. Im, J.-H., Lee, C.-R., Lee, J.-W., Park, S.-W. & Park, N.-G. *Nanoscale* **3,** 4088–4093 (2011).
15. Chung, I., Lee, B., He, J., Chang, R. P. H. & Kanatzidis, M. G. *Nature* **485,** 486–489 (2012).
16. Kim, H.-S. *et al. Sci. Rep.* **2,** 591 (2012).
17. Lee, M. M., Teuscher, J., Miyasaka, T., Murakami, T. N. & Snaith, H. J. *Science* **338,** 643–647 (2012).
18. Etgar, L. *et al. J. Am.Chem. Soc.* **134,** 17396–17399 (2012).
19. Mei, A. *et al. Science* **345,** 295–298 (2014).
20. Heo, J. H. *et al. Nature Photon.* **7,** 487–492 (2013).
21. Liu, M., Johnston, M. B. & Snaith, H. J. *Nature* **501,** 395–398 (2013).
22. Malinkiewicz, O. *et al. Nature Photon.* **8,** 128–132 (2014).
23. Burschka, J. *et al. Nature* **499,** 316–319 (2013).
24. Chen, Q. *et al. J. Am. Chem. Soc.* **136,** 622–625 (2014).
25. Yella, A., Heiniger, L.-P., Gao, P., Nazeeruddin, M. K. & Grätzel, M. *Nano Lett.* **14,** 2591–2596 (2014).
26. Jeon, N. J. *et al. Nature Mater.* **13,** 897–903 (2014).
27. Juarez-Perez, E. J. *et al. J. Phys. Chem. Lett.* **5,** 2390–2394 (2014).
28. Dualeh, A. *et al. ACS Nano* **8,** 362–373 (2014).
29. Pellet, N. *et al. Angew. Chem. Int. Ed.* **53,** 3151–3157 (2014).
30. Grätzel, M. *Nature* **414,** 332–344 (2001).
31. Xing, G. *et al. Nature Mater.* **13,** 476–480 (2014).
32. Deschler, F. *et.al. J. Phys. Chem. Lett.* **5,** 1421–1426 (2014).
33. Ross, R. T. *J. Chem. Phys.* **46,** 4590 (1967).
34. Hao, F., Stoumpos, C. C., Cao, D. H., Chang, R. P. H. & Kanatzidis, M. G. *Nature Photon.* **8,** 489–494 (2014).
35. Noel, N. K. *et al. Energy Environ. Sci.* http://dx.doi.org/10.1039/c4ee01076K (2014).
36. Kumar, M. H. *et al. Adv. Mater.* (in the press).
37. Ito, S. *et al. Thin Solid Films* **516,** 4613–4619 (2008).

Acknowledgements

I am grateful to my co-workers at the Laboratory of Photonics and Interfaces at EPFL, and to all academic partners with whom I have cooperated in the field of perovskite solar cells, in particular N.-G. Park, (SKKU Korea), S. I. Seok (KRICT Korea), S. Mhaisalkar, N. Mathews and T. C. Sum (NTU Singapore), H. W. Han (HUST China) and H. Bolink (Univ. of Valencia Spain). Financial support by the Swiss National Science Foundation and the European Research Council through the Advanced Research Grant (ARC no. 247404) 'Mesolight' and the Global Research Laboratory (GRL) programme, funded by the National Research Foundation in Korea are specifically acknowledged.